Hybrid modelling based control of an processing/reprocessing mechatronics line served by an autonomous robotic system*

G. Petrea, A. Filipescu, A. Filipescu Jr., A. Serbencu
Department of Automation and Electrical Engineering,
"Dunarea de Jos" University of Galati
Galati, Romania
george_petrea@hotmail.com
adrian.filipescu@ugal.ro
adriana.filipescu@ugal.ro
adriana.serbencu@ugal.ro

Eugenia Minca
Department of Automation, Computer Science and Electrical Engineering
"Valahia" University of Targoviste
Targoviste, Romania

Alina Voda
"Joseph Fourier" University 1/CNRS, -GIPSA-lab,
Grenoble, France

***Abstract* – The new idea in this paper is to make a processing line capable of reprocessing pieces that have not passed the quality test. The focus is to provide a model of the processing line and to introduce in the process a wheeled mobile robot (WMR) equipped with a robotic manipulator (RM) in order to transport pieces, for reprocessing. For this purpose, an processing/reprocessing mechatronics line (P/RML) and a timed hybrid Petri nets (THPN) model will be used in modeling and control of the mechatronics line, with a fixed number of workstations, served by a WMR equipped with (RM). The THPN model is a hybrid type, where P/RML is the discrete part and WMR with RM is the continuous part. The reprocessing starts after the piece fails the quality test. The WMR with RM is used only at the start of reprocessing, in order to transport the pieces from the warehouse to the beginning of the processing line.**

Keywords- mechatronics, Hybrid Petri nets, mobile robot

I. INTRODUCTION

In the last decade the industry is put in front of a new global evolution, driven by the technological progress. This improvement is extended in all industrial domains and triggers the evolution of new generations of advanced flexible production systems and new methods of centralized management distributed or supervised. Also this involves the evolution of new types of robots and processing machine tools and the need of efficient transport and manipulation systems [1], [2], [3].

Flexibility and process optimization have drawn the attention of the researches in this field. Most of the studies are based on the increase of the number of manufacturing operations with the same equipment and productivity growth, both having an impact on the quality of the final product [4], [5]. It is well known that the quality of the product and the manufacturing process are tightly bounded. In [6] flexibility characteristic and its impact on performance growth of the flexible manufacturing systems is analysed. In flexible manufacturing systems appear parallel asynchronous events (time parallelism), also known as concurrent asynchronous events.

Since these asynchronous events tend to achieve a common goal, that of the whole aggregate operation, these events coincide in time intervals that occur [7], [8].

Such asynchronous parallel events in flexible manufacturing systems can be simultaneous processing of parts on various stations (machine tools), made simultaneously with transport and/or handling of parts to (or from) other stations with the execution of different operations (processing, assembly, disassembly). These events are asynchronous because a synchronization system of this large number of events does not exist.

Such a system could not be achieved, taking into account the complexity of the flexible manufacturing system and the fact that events do not unfold exactly according to predetermined sequences, but as a result of successive conditionings, that do not have invariableness character and the relative velocities of events developing could not be known beforehand.

The existence of parallel asynchronous events require complex modeling techniques adopted for driving a flexible manufacturing system and the relatively small number of techniques used to date has been determined by this inconvenience, and the requirements imposed to the model: generality of application, ease of use and representation fidelity.

In this paper the main objective is the modelling and simulation of FESTO MPS-200 processing system dynamics at the occurrence of events using a THPN model. Also it is shown an approach on the simulation of the mobile platform Pioneer P3-DX when serving the FESTO processing system.

*This work was supported by UEFISCDI, project number PN-II-ID-PCE-2011-3-0641.

978-1-4799-2228-4/13/$31.00 ©2013 IEEE

II. Initial Conditions

The mechatronics system FESTO MPS-200 is a flexible teaching line for processing, sorting and storage. It is composed of 4 stations (cells), each performing different operations.

When asynchronous events appear the Pioneer P3-DX mobile robot equipped with a robotic arm intervenes in the process and transports the parts from the storage station. In the analysis and modeling of the flexible processing line FESTO MPS-200 (fig. 1) are introduced initial operating assumptions regarding the process.

Pieces stored on the upper level of the storage are considered scrap pieces and will be put back on line for a new flexible machining operation. Bringing of the declared scrap parts to the processing line again is done using the mobile robot equipped with a manipulator. In fig.1 are presented the sections and trajectories which the mobile platform equipped with manipulator makes in the process of servicing the flexible manufacturing line FESTO MPS-200, where:

R_L^1 represents the number and position of the location where the mobile robot equipped with manipulator is set in the process of taking the piece;

R_L^2: represents the number and position of the location where the mobile robot equipped with manipulator is set in the process of depositing the piece;

T_L^1 is the number of the location to store the piece so that it could be taken by the mobile robot equipped with a manipulator;

T_L^2 is the number of the location into which the piece is deposited by the WMR equipped with RM for a new processing operation.

Considering the analysis described in the previous section in fig. 3 is proposed the planning of tasks related to flexible line FESTO MPS-200.

Strategies for sorting, processing and storage are based on a graph representation of the processed product where relations between the stations are expressed by arrows. Using this graph is developed a planning of the tasks which will determine the sequence in which the components are processed.

If a component is not validated at the color test or has been validated tasks planning provides the best sequence to perform its processing and storage in the warehouse.

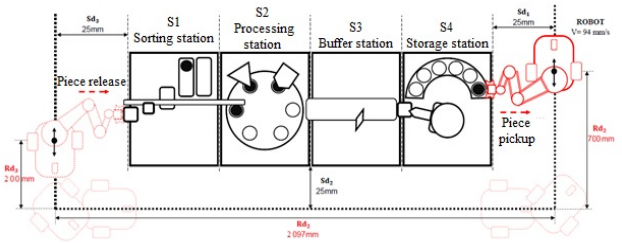

Figure 1. Division into sections and path passed by the mobile robot

III. Modeling of the Mechatronic Processing Line

Using Petri Nets in modeling the processing/reprocessing line FESTO MPS-200 will permit that the models obtained to be correlated with the real time evolution of the process.

There are some notations to be made:

$$P_{dp} = \{P_{dp_1}, \quad P_{dp_2}, \quad \ldots. \quad P_{dp_n}\} \tag{1}$$

$$P_{dp} = \{P_{dp_i}\}_{i=\overline{1,13}} \tag{2}$$

where: $\{P_{dp_i}\}_{i=\overline{1,13}}$ is the set of locations for processing operation.

$$T_{dp} = \{T_{dp_1}, \quad T_{dp_2}, \quad \ldots. \quad T_{dp_n}\} \tag{3}$$

$$T_{dp} = \{T_{dp_i}\}_{i=\overline{1,12}} \tag{4}$$

where: $\{T_{dp_i}\}_{i=\overline{1,12}}$ is the set of transitions for processing operation;

Considering the task planning in fig. 2 and the process description in section 2, the timed Petri Net represents the model of the flexible line, model outlining the actual process of machining in discrete event system approach.

During processing, the timed transitions are:

$T_{dp2} = 0$, $T_{dp3} = 0$, $T_{dp9} = 0$ and $T_{dp10} = 0$ are assigned a value of zero, since each transition corresponds to a state of process that happens instantly;

$$T_{dp1} = 3.5s\,; T_{dp4} = 6.9s\,; T_{dp5} = 4.8s\,; T_{dp6} = 3.9s\,;$$

$$T_{dp7} = 3.4s\,; T_{dp8} = 10.9s\,; T_{dp11} = 11.8s\,; T_{dp12} = 13.3s$$

To develop a global model of processing and reprocessing will consider hybrid aspect of the process served by platform. In modeling will be used Timed Hybrid Petri Nets (THPN)) which integrates the discrete appearance of the process together with the continuous appearance of the moving of WMR.. The THPN model describes the following automatic operations:

- Processing/reprocessing pieces (TPN typology);
- Transporting defective pieces for reprocessing (THPN typology).

The continuous places of the model represent the 3 distances in which the path from the warehouse to the beginning point of the processing line is divided. Because it is not a linear trajectory, the robot has to make 2 90° turns, which are modeled as discrete actions. The speed of the robot and the distances imposed the parameters of the hybrid model, and the delays for the discrete states are the ones measured in real time.

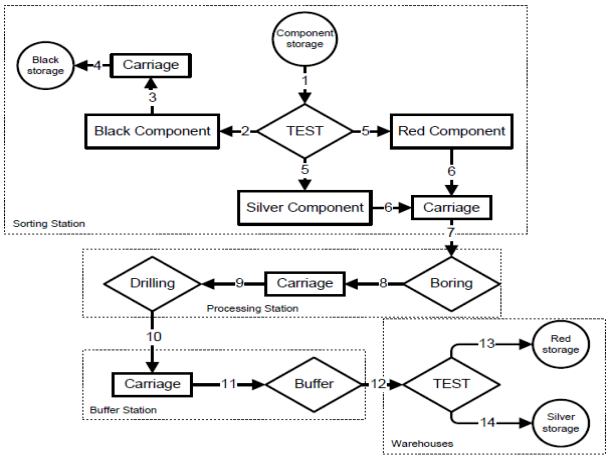

Figure 2. Task planning for sorting, reaming, drilling and storage operations

In the case of Hybrid Petri Nets approach $THPN$ is a septuplet:

$$THPN = \langle P, T, Pre, Post, m_0, h, tempo \rangle \tag{5}$$

$$P = P_d \cup P_c \tag{6}$$

is a finite, not empty, set of places where P_d is the set of discrete places

$$P_d = \{P_{dp_i}\}_{i=\overline{1,13}} \cup \{P_{dr_j}\}_{j=\overline{1,8}} \tag{7}$$

and P_c the set of continuous places

$$P_c = \{P_{cr_k}\}_{k=\overline{1,3}}. \tag{8}$$

$$T = T_d \cup T_c \tag{9}$$

is a finite, not empty, set of transitions where T_d is the set of discrete transitions

$$T_d = \{T_{dp_i}\}_{i=\overline{1,12}} \cup \{T_{dr_j}\}_{j=\overline{1,11}} \tag{10}$$

and T_c the set of continuous transitions

$$T_c = \{T_{cr_k}\}_{k=\overline{1,3}} \tag{11}$$

Remark 1: Sets P and T are disjointed, $P \cap T = \varnothing$;

$Pre: P \times T \to Q_+$ or N is the input incidence application;

$Post: P \times T \to Q_+$ or N is the output incidence application;

Remark 2: In the definitions of Pre, $Post$ and m_0, N corresponds to the case where $P_i \in P_d$, and Q_+ or R_+ corresponds to the case where $P_i \in P_c$.

$m_0: P \to R_+$ or N is the initial marking;

$$h: P \cup T \to \{D, C\}, \tag{12}$$

called a "hybrid function", indicates for every node whether it is a discrete node (sets P_d and T_d) or a continuous node (sets P_c and T_c),

$$h: P_d \cup T_d \to \{D\}; h: P_c \cup T_c \to \{C\}, \tag{13}$$

tempo is a function from the set T of transitions to the set of positive or zero rational numbers,

$$tempo: T \to Q_+ \cup \{0\}. \tag{14}$$

If $T_j \in T_d$, then $d_j = tempo(T_j)$ is the timing associated with T_j.

If $T_{cr} \in T_c$ then

$$U_r = \frac{1}{tempo(T_{cr})} \tag{15}$$

is the flow rate associated with T_{cr}.

For $T_c = \{T_{cr_k}\}_{k=\overline{1,3}}, U_{cr_k} = U_r; U_{r\max} = V_r$, where U_{cr} is the variable flow of mobile robot displacement between continuous places. Consider the average speed of motion of WMR, $V_r = 94 mm/s$.

In fig. 16 it is shown the THPN model obtained for the processing/reprocessing line, regarding the assumptions made above. Next, in fig.3 the simulated response of the continuous places of WMR for the hybrid model from fig.16. are shown. The WMR markings of the continuous places, before and after simulation match the distances shown in fig.1.

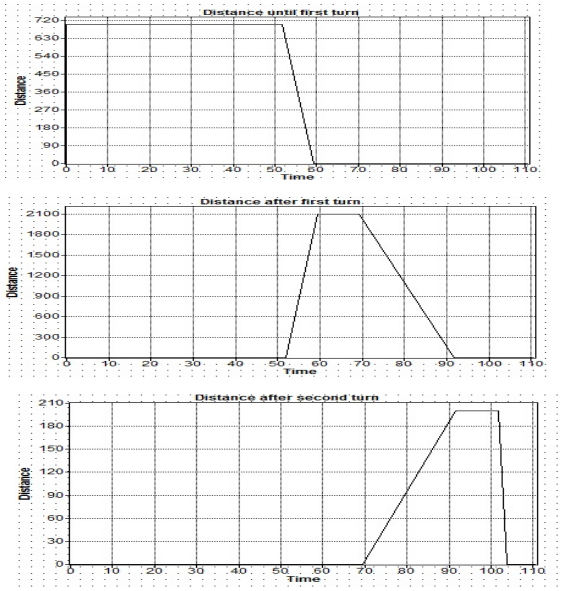

Figure 3. Variation of the continuous places associated to displacements of WMR with RM for the transporting stage

IV. Real-Time Control of WMR Serving Mechatronics Processing Line

Discrete-time sliding-mode control for trajectory-tracking, based on a kinematic model is used in order to control WMR Pioneer 3-DX. Pioneer 3-DX is a mobile platform with two driving wheels and one rear wheel. The robotic manipulator, Pioneer 5-DOF Arm, mounted on the mobile platform, is controlled in open loop by step by step motors located in each joint. The gripper positioning in order to grab the scrap piece in the warehouse has been made by a visual servoing system.

A. Kinematic Model of the Mobile Platform

The mobile platform has two differential drive wheels and a guiding wheel as shown in fig. 4.

Kinematics modeling of mobile platforms issue was explicitly addressed in the literature [9], [10]:

$$\begin{cases} \dot{x}_r = v_r \cdot \cos\theta_r \\ \dot{y}_r = v_r \cdot \sin\theta_r \\ \dot{\theta}_r = \omega_r \end{cases} \tag{16}$$

where x_r and y_r are Cartesian coordinates of the geometric center of the mobile platform, v_r is the linear velocity of the mobile platform, θ_r is the steering angle, angular velocity of the robot is ω_r and b is the distance between the planes of the driving wheels.

B. Sliding Mode Driving of the Mobile Platform

Trajectory tracking errors can be characterized by $(x_e,\ y_e,\ \theta_e)$. The purpose of this section is to design a stable controller, which generates a control vector $(v_c,\ \omega_c)$. Trajectory tracking error vector is:

$$\begin{bmatrix} x_e \\ y_e \\ \theta_e \end{bmatrix} = \begin{bmatrix} \cos\theta_d & \sin\theta_d & 0 \\ -\sin\theta_d & \cos\theta_d & 0 \\ 0 & 0 & 1 \end{bmatrix} \cdot \begin{bmatrix} x_r - x_d \\ y_r - y_d \\ \theta_r - \theta_d \end{bmatrix} \tag{17}$$

where, (x_d, y_d, θ_d) is the virtual position of the mobile platform. The derived of the tracking error can be written,

$$\begin{cases} \dot{x}_e = -v_d + v_r \cdot \cos\theta_e + \omega_d \cdot y_e \\ \dot{y}_e = v_r \cdot \sin\theta_e - \omega_d \cdot x_e \\ \dot{\theta}_e = \omega_r - \omega_d \end{cases} \tag{18}$$

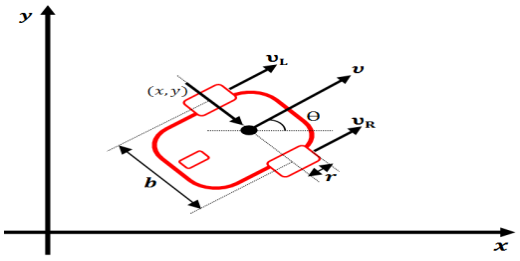

Figure 4. Kinematic variables of the mobile platform with two driving wheels and a rear free wheel.

where, v_d and ω_d are the desired linear and angular velocities. Here it is supposed that $|\theta_e| < \pi/2$ which implies that the orientation of the mobile platform should not be perpendicular to the desired direction. A new sliding surface was introduced so that the lateral error, y_e, and the angular variable, θ_e, are internally connected in the same area and both variables converge to zero. For this purpose the following areas have been defined:

$$\begin{cases} s_1 = \dot{x}_e + k_1 \cdot x_e \\ s_2 = \dot{y}_e + k_2 \cdot y_e + k_0 \cdot \mathrm{sgn}(y_e) \cdot \theta_e \end{cases} \tag{19}$$

where, k_1, k_2, k_3 are positive constant parameters, x_e, y_e and θ_e are the tracking errors defined in equation (16).

If surface s_1 converges to zero, x_e converges to zero. If s_2 converges to zero, then y_e becomes

$$\dot{y}_e = -k_2 \cdot y_e + k_0 \cdot \mathrm{sgn}(y_e) \cdot \theta_e \tag{20}$$

If $y_e > 0$ and $k_0 < k_2 \cdot |y_e| / |\theta_e|$ then $\dot{y}_e < 0$. Finally it is known from s_2 that the convergence of y_e and $\dot{y}_e$ lead to the convergence of θ_e to zero.

The general practical driving law form is:

$$\dot{s} = -Q \cdot \mathrm{sgn}(s) - P \cdot s \tag{21}$$

where Q and Q are positive constants. Adding the term $-Qs$, the state is forced to fast approach the switching zone when s is large. Knowing that:

$$\dot{\theta}_e = \dot{\theta}_r - \dot{\theta}_d = \dot{\omega}_r - \dot{\omega}_d \tag{22}$$

Then, after the derivation of (19) and (20), it is obtained:

$$\dot{v}_c = \begin{pmatrix} -Q_1 sign(s_1) - P_1 s_1 - k_1 \dot{x}_e - \dot{\omega}_d y_e \\ -\omega_d \dot{y}_e + v_r \dot{\theta}_e \sin\theta_e + \dot{v}_d \end{pmatrix} \Big/ \cos\theta_e \tag{23}$$

$$\omega_c = \begin{pmatrix} -Q_2 sign(s_2) - P_2 s_2 - k_2 \dot{y}_e \\ -\dot{v}_r \sin\phi_e + \dot{\omega}_d x_e + \omega_d . \dot{x}_e \end{pmatrix} \Big/ \begin{pmatrix} v_r \cos\phi_e \\ +k_0 \mathrm{sgn}(y_e) \end{pmatrix} + \omega_d \tag{24}$$

The Lyapunov function is defined $V = \frac{1}{2} \cdot s^T \cdot s$, so the derivative in time is

$$\begin{aligned} \dot{V} = s_1 \cdot \dot{s}_1 + s_2 \cdot \dot{s}_2 = s_1 \cdot \left(-Q_1 \cdot \mathrm{sgn}(s_1) - P_1 \cdot s_1\right) \\ + s_2 \cdot \left(-Q_2 \cdot \mathrm{sgn}(s_2) - P_2 \cdot s_2\right) \end{aligned} \tag{25}$$

In order to have a negative and semi defined $\dot{V}$ it is enough to choose Q_i and P_i $i \in \{1,2\}$ so that $Q_i, P_i \geq 0$. Closed loop sliding-mode control of the WMR is shown in fig. 5. Using the above discussed equations, in the real time simulation, the trajectory passed by the Pioneer P3-DX robot along with the flexible line FESTO MPS-200 is shown in fig.

6. Before the simulation, some conditions had to be imposed: the total distance traveled by the mobile platform is 5834 mm; the path is crossed over in two stages: retrieval-deposit and return to the initial position.

C. Results via Simulation and Real Time Control

Figure 7 shows the 3 kind of work pieces involved in the processing and the movement of the robot at the appearance of a defective piece. In fig. 8, it is shown the real and the imposed trajectories of the mobile platform. Both trajectories coincide on all distance passed. When the platform turns 90^0 a small deviation from the trajectory can be noticed. In fig. 9 are noticed variations of the real linear speed regarding the imposed speed From simulation has resulted that the necessary time for the mobile platform to pass the 5834 mm distance was of 121.7 s. In fig. 10 is shown the tracking error on x axis. The maximum error consists of a 4 mm deviation of the mobile robot regarding the imposed distance. In fig. 11 it is shown the tracking error on y axis which has a maximum of 2 mm.

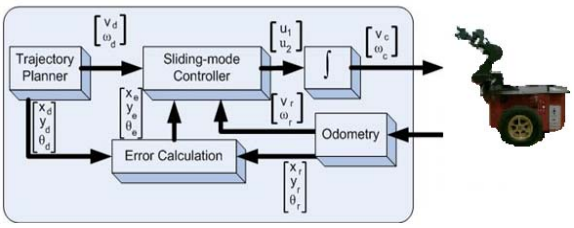

Figure 5. Closed loop WMR control

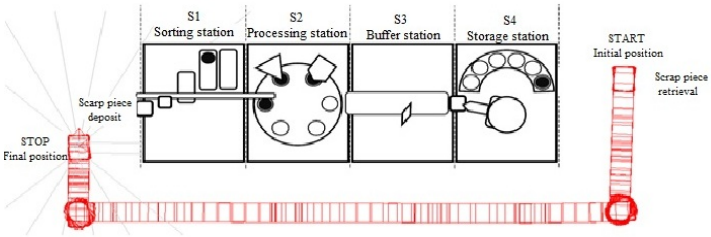

Figure 6. WMR simulated response in trajectory tracking sliding mode control serving processing line FESTO MPS-200.

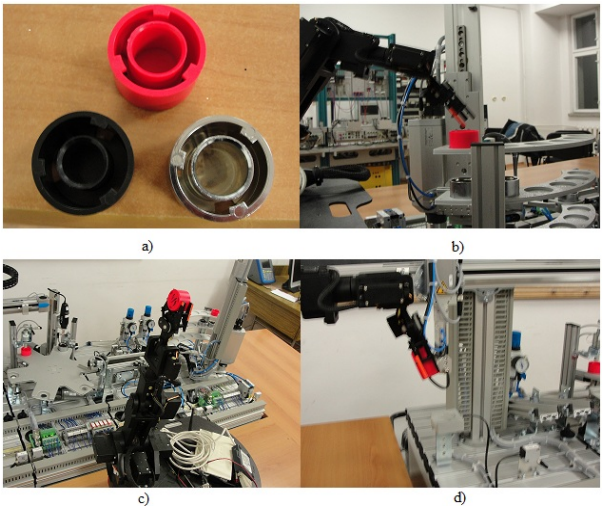

Figure 7. a) Types of pieces; b), c) and d) WMR, Pioneer P3-DX, with RM, Pioneer 5-DOF, serving FESTO MPS-200.

When the robot makes last 90^0 turn, the deviation reaches its maximum of 2.37 mm. In fig.12 it is shown the orientation error of the mobile platform which is of approximately 2^0 and in fig. 13 are shown the desired and the real angular speed, with an error between them of 0.5 rad/s. In fig. 14 and 15 are shown the commands for sliding mode driving of the mobile platform in s_1 and s_2 surfaces.

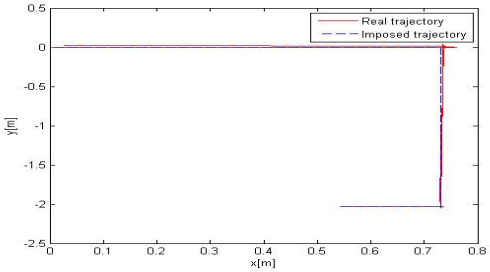

Figure 8. Imposed vs real trajectories of the WMR

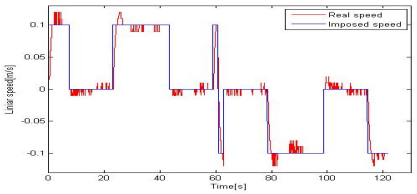

Figure 9. Imposed vs real linear speeds of the WMR

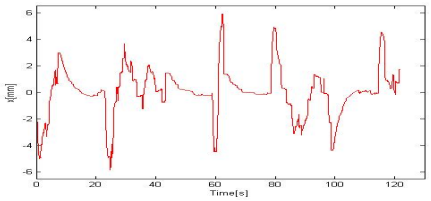

Figure 10. X axis tracking error of the WMR

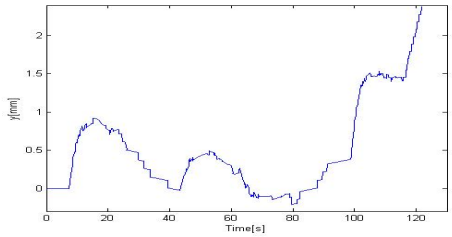

Figure 11. Y axis tracking error of the WMR

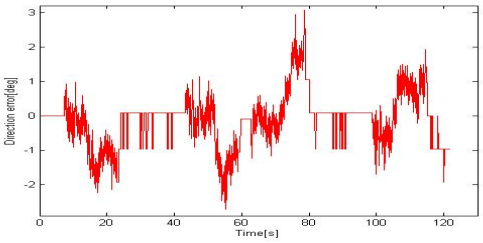

Figure 12. Orientation error of the WMR

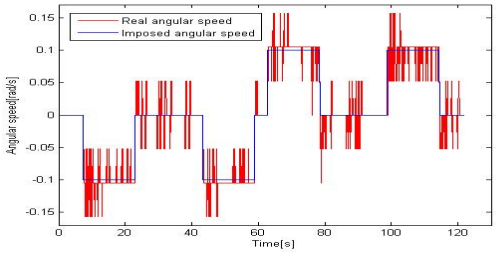

Figure 13. Imposed vs real angular speed of the WMR

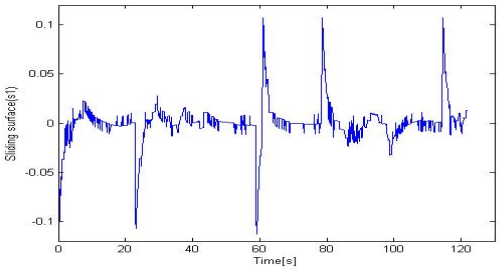

Figure 14. Control input on sliding surface

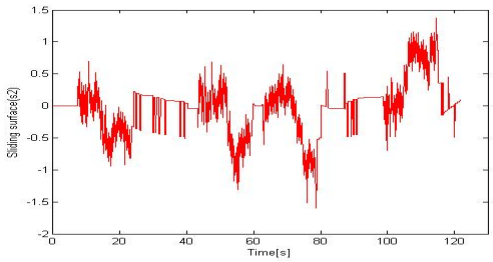

Figure 15. Control input on sliding surface

V. CONCLUSIONS

The main contribution of this paper is the optimization and management of the flexible processing line. In order to do that, were implemented different driving programs for the line and models with timed, non-timed and hybrid Petri Nets. The chosen modeling represents a good solution for accurately highlight the real process and to show different properties of the discreet event system. Validating the simulation model can produce a limited set of states of the modeled system and thus can only show the presence (but not absence) of errors in the model and its basic specifications. In the simulation of the processing served by a mobile robot equipped with a manipulator for the flexible line FESTO MPS-200 were eliminated errors, unwanted situations and events. In the simulation values were used for state transitions in real process of simulation to better reflect the behavior of flexible lines.

REFERENCES

[1] Toni A. and Tonchia S. *Manufacturing Flexibility: a literature review.* International Journal of Production Research, 1998, vol. 36, no. 6, 1587-617.

[2] Chryssolouris G. *Manufacturing Systems – Theory and Practice.* New York, NY: Springer Verlag, 2005. 2nd edition.

[3] Tolio D., *Design of Flexible Production Systems – Methodologies and Tools*. Berlin: Springer, 2009. ISBN 978-3-540-85413-5.

[4] F.F. Chen and E.E. Adams, *"The Impact of Flexible Manufacturing Systems on Productivity and Quality"*, IEEE Transactions of Engineering Management, vol. 38, pp. 33-45, 1991.

[5] G. Da Silverira, D. Borenstein and F.S. Fogliatto, *"Mass Customization: Literature Review and Research Directions"*, International Journal of Production Economics, vol. 72, pp. 1-13, 2001.

[6] A. Radaschin, A. Voda, E. Minca, A. Filipescu, *"Task Planning Algorithm in Hybrid Assembly/Disassembly Process"*, 14th IFAC Symposium on Information Control Problems in Manufacturing, May 23-25, 2012, Bucharest, ISSN: 1474-6670; ISBN: 978-3-902661-98-2, pp. 571-576.

[7] A. Filipescu, S. Filipescu, E. Minca, *"Hybrid System Control of an Assembly/Disassembly Mechatronic Line Using Robotic Manipulator Mounted on Mobile Platform"*, The 7th IEEE Conference on Industrial Electronics and Applications (ICIEA2012), 18-20 July,2012, Singapore, pp. 433-438, IEEE Catalog Number CFP 1220A-CDR, ISBN: 978-1-4577-2117-5

[8] E. Minca, A. Filipescu and A. Voda *"New Approach in Control of Assembly/Disassembly Line Served by Robotic Manipulator Mounted on Mobile Platform,* 2012 IEEE International Conference on Robotics and Biomimetics (ROBIO 2012), ISBN;978-1-4673-2126-6, pp.235-240, 11-14 Dec, 2012, Guangzhou, China.

[9] Fukao T., Nakagawa H., Adachi N., *Adaptive tracking control of a nonholonomic mobile robot*, IEEE Transactions on Robotics and Automation, vol. 16, nr.5, pag. 609-615, 2000.

[10] De Luca A. and Oriolo G. (1995). *Modelling and Control of Nonholonomic Mechanical Systems*, in: J. Angeles, A. Kecskemethy (Editors), Kinematics and Dynamics of Multi-Body Systems, Springer-Verlag, 277–342.

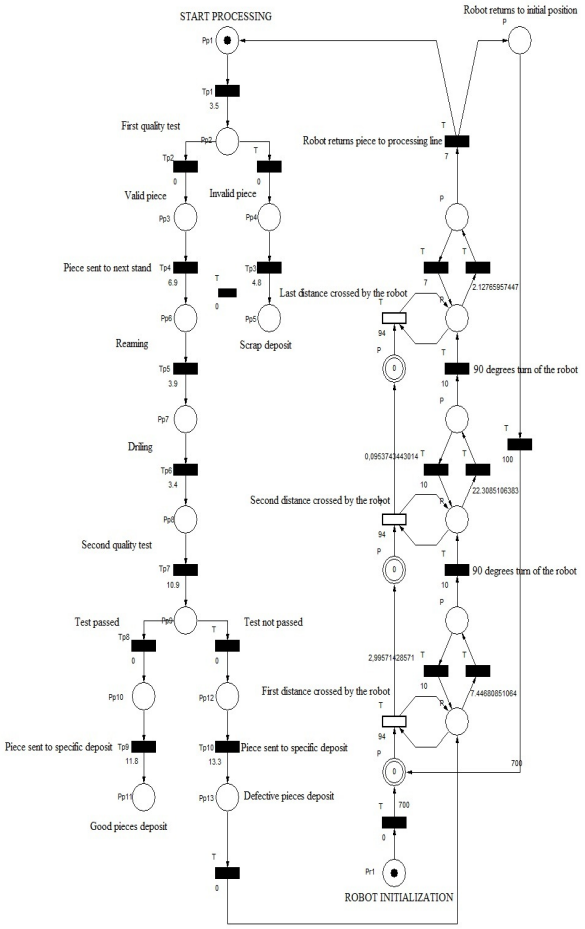

Figure 16. THPN model of processing/reprocessing line served by WMR equipped with RM.